Identification and Thermodynamic Characterization of Molten Globule States of Periplasmic Binding Proteins†

Ravindra Singh Prajapati,‡ S. Indu,‡ and Raghavan Varadarajan*,‡,§

Molecular Biophysics Unit, Indian Institute of Science, Bangalore 560 012, India, and Chemical Biology Unit, Jawaharlal Nehru Center for Advanced Scientific Research, Jakkur, P.O., Bangalore 560 004, India

Received March 26, 2007; Revised Manuscript Received June 26, 2007

ABSTRACT: Molten globule-like intermediates have been shown to occur during protein folding and are thought to be involved in protein translocation and membrane insertion. However, the determinants of molten globule stability and the extent of specific packing in molten globules is currently unclear. Using far- and near-UV CD and intrinsic and ANS fluorescence, we show that four periplasmic binding proteins (LBP, LIVBP, MBP, and RBP) form molten globules at acidic pH values ranging from 3.0 to 3.4. Only two of these (LBP and LIVBP) have similar sequences, but all four proteins adopt similar three-dimensional structures. We found that each of the four molten globules binds to its corresponding ligand without conversion to the native state. Ligand binding affinity measured by isothermal titration calorimetry for the molten globule state of LIVBP was found to be comparable to that of the corresponding native state, whereas for LBP, MBP, and RBP, the molten globules bound ligand with approximately 5−30-fold lower affinity than the corresponding native states. All four molten globule states exhibited cooperative thermal unfolding assayed by DSC. Estimated values of ΔC_p of unfolding show that these molten globule states contain 28−67% of buried surface area relative to the native states. The data suggest that molten globules of these periplasmic binding proteins retain a considerable degree of long range order. The ability of these sequentially unrelated proteins to form highly ordered molten globules may be related to their large size as well as an intrinsic property of periplasmic binding protein folds.

Protein folding is a process by which a disordered polypeptide chain folds into a specific structure (native), which shows biological activity. It has been previously postulated (*1*, *2*) that a protein folds first into a rather flexible state, which exhibits native-like mutual positions of α-helices and *β*-strands. However, it lacks tight packing of side chains, and the protein acquires its tertiary structure at the end of the folding process. The first evidence for this kind of equilibrium intermediate during protein unfolding came from chemical (GdmCl[1])-induced denaturation of carbonic anhydrase (*3*). The far- and near-UV CD spectra of this intermediate showed a loss in tertiary structure while retaining the native-like secondary structure state (*3*). Similar observations were made for acid- and temperature-induced unfolding (*4*, *5*). Similar kinds of equilibrium and kinetic intermediates were also observed in other proteins (*4*, *6*, *7*), and these states were referred to as molten globules (*8*). The term molten globule applies to all compact denatured states that have native-like secondary structure but little or no fixed tertiary structure. This covers a wide range of more or less disordered and partially folded proteins, with or without disulfide bonds (*9*−*11*). The molten globule state has been asserted to be a third state of proteins, which is different from the native and unfolded states (*12*). Detailed structural information on molten globules is, however, scarce. A study on a truncated form of staphylococcal nuclease in a non-native state, using a conformation-dependent chemical cleavage technique, indicated that the backbone was adopting a native-like fold, although there were some regions that had a non-native structure (*13*). Another study on urea-induced non-native conformations of staphylococcal nuclease by NMR suggested a native-like spatial positioning and orientation of chain segments (*14*).

The presence of the molten globule state has also been confirmed in living cells, and it is believed to occur during *in vivo* protein folding in some cases (*15*, *16*). This state has also been implicated in genetic diseases, such as cystic fibrosis (*17*−*20*) and emphysema (*17*, *21*−*23*). Several studies have demonstrated that chaperones can interact with molten globule states to prevent their aggregation (*24*), reconstitute enzyme activity (*25*), and mediate protein folding (*26*, *27*). Molten globule-like intermediates are suggested to be involved in the translocation and insertion of proteins in the plasma membrane and other intracellular membranes (*28*−*31*). Molten globule states are also found as both equilibrium and kinetic intermediates during protein folding

† This work was supported by grants from Department of Biotechnology, Government of India and The Wellcome Trust.

* Corresponding author. Phone: 91-80-22932612. Fax: 91-80-23600535. E-mail: varadar@mbu.iisc.ernet.in.

‡ Indian Institute of Science.

§ Jawaharlal Nehru Center for Advanced Scientific Research.

[1] Abbreviation: LBP, leucine binding protein; LIVBP, leucine/isoleucine/valine binding protein; MBP, maltose binding protein; RBP, ribose binding protein; ANS, 8-anilino1-naphthalene sulfonic acid; WT, wild type; MG, molten globule state; N, native state; U, unfolded state; CGH10, 10 mM sodium citrate, 10 mM glycine, and 10 mM HEPES; CD, circular dichroism; UV, ultra violet; ASA, accessible surface area; DSC, differential scanning calorimetry; ITC, isothermal titration calorimetry; GdmCl, guanidinium chloride.

10.1021/bi700577m CCC: $37.00
Published on Web 08/15/2007

in vitro (*4*, *8*, *11*). It has also been observed that in some cases kinetic and equilibrium molten globule states for a given protein have similar properties (*32*). Molten globule states are stabilized by acidic pH and high salt concentrations (*33*, *34*). Thermodynamic properties of molten globule states have been characterized for a few proteins. In certain cases such as in human α-lactalbumin, unfolding of molten globule states is accompanied by small or zero values of ΔH and ΔC_p (*35*−*39*). In contrast, unfolding of the molten globule states of MBP and yeast iso-1-cyt *c* showed significant ΔC_p and ΔH (*40*, *41*). The nature of interactions stabilizing molten globules and the extent of specific tertiary packing present in molten globules are still not well understood. It is also currently unclear whether the ability to form molten globules is an intrinsic property of the fold or whether it depends on the specific sequence of the protein. Most studies on molten globules have been on relatively small proteins, typically less than 20 kDa, many of which contain disulfides, metal ions, or prosthetic groups in the native state. In addition, typically only a single member of a fold is characterized. There are few reports, describing molten globules of larger proteins, possibly because larger proteins typically do not show reversible folding and are prone to aggregation.

Given the potential involvement of molten globule states in protein translocation and the relatively limited thermodynamic information available on determinants of molten globule stability, we have identified and characterized molten globule states for leucine binding protein (LBP), leucine/isoleucine/valine binding protein (LIVBP), maltose binding protein (MBP), and ribose binding protein (RBP). These are relatively large (36.98, 36.77, 40.70, and 28.47 kDa, respectively), monomeric, two-domain proteins found in the periplasm of *E. coli*. They are involved in the binding and transport of leucine, leucine/isoleucine/valine, maltose, and ribose, respectively. We find that the molten globule states for these four proteins show reversible thermal transitions, are likely to be well ordered, and bind to their ligands with comparable (LBP) or with slightly lower (LIVBP, MBP, and RBP) affinity than that of their corresponding native states.

MATERIALS AND METHODS

Materials. L-Leucine, L-isoleucine, L-alanine, D-(−)-maltose, D-(+)-ribose, D-(+)-glucose, sucrose, IPTG, ampicillin, sodium citrate, ANS, Tris, glycine, and urea were from Sigma Aldrich. HEPES and Q-Sepharose were from USB (Amersham Life Sciences). Other chemicals were from local commercial sources and were of analytical grade. Origin and Sigma plot software were used for data analysis. All the studies were carried out in CGH10 (citrate, glycine, and HEPES, 10 mM each) buffer except for far-UV CD spectra acquisition, which was carried out in CGH5.

Strains, Plasmids, and Protein Purification. The genes encoding MBP and RBP cloned in plasmids pMALp2MBP and pCMB1 were used for the expression of corresponding proteins in *E coli* DH5α (*42*). The plasmids pKSty and pJSty carrying the genes for LBP (a kind gift from Dr. L. Luck (*43*)) and LIVBP (*44*), respectively, under the control of the T7 promoter were expressed in *E coli* BL21 (DE3). Cells were grown in LB medium containing 100 mg/L ampicillin at 37 °C. The culture was induced with 0.1 mM IPTG at an OD_{600} of 0.8. After 6 h of incubation, cells were pelleted at 6000 rpm. Following osmotic shock (*42*) to extract proteins from periplasmic regions, ion-exchange chromatography was carried out on a Q-Sepharose fast flow column using a 0.0−0.5 M NaCl gradient in 10 mM Tris at pH 8.0 at 4 °C. LBP, LIVBP, MBP, and RBP elute at approximately 170 mM, 140 mM, 75 mM, and 70 mM NaCl, respectively.

Protein purity was assessed by Coomassie staining following SDS−PAGE. All of the proteins were found to be >95% pure. Protein concentration was estimated using extinction coefficients of 41,100, 35,600, 65,370, and 4350 M^{-1} cm^{-1} at 280 nm for LBP, LIVBP, MBP, and RBP, respectively. The extinction coefficients for LIVBP, RBP, and MBP are identical to those described previously (*42*, *45*), and those for LBP, were calculated as described (*46*). Approximate yields of purified proteins were 20, 20, 25, and 40 mg /L for LBP, LIVBP, MBP, and RBP, respectively.

Far-UV CD Measurements. All CD measurements were carried out on a JASCO J-715A Spectrometer. Far-UV CD spectra were acquired at different pH values of 1.0, 2.0, 3.2, 3.4, 3.6, 3.8, 4.0, and 7.0 for all four proteins in the wavelength range of 200−250 nm. All protein samples were incubated for 2 to 3 h at 25 °C before measurement. The concentrations of the samples were 8−10 μM. Measurements were recorded in a 1 mm path length quartz cuvette with a scan rate of 50 nm/min, a response time of 4 s, and a bandwidth of 2 nm. Each spectrum was an average of four consecutive scans. Buffer spectra were also acquired under similar conditions and subtracted from protein spectra, before analysis.

Near-UV CD Measurements. Near-UV CD measurements were carried out for native (pH 8.0 for LBP; pH 7.0 for LIVBP and MBP) and molten globule states (pH 3.4 for LBP; pH 3.0 for LIVBP and MBP) of LBP, LIVBP, and MBP in the presence and in the absence of leucine, isoleucine, and maltose, respectively. Samples were incubated at 25 °C for 2 to 3 h, the respective ligand was then added, and the samples were further incubated for 30 min. Spectra were acquired over the wavelength range of 250−310 nm with 40 μM protein and 1 mM ligand (for all four proteins) in a 1 mm path length quartz cuvette; other conditions were similar to those for far-UV CD spectra. Each spectrum was an average of four consecutive scans. Buffer spectra were also acquired under similar conditions and subtracted from protein spectra, before analysis.

Isothermal Equilibrium Unfolding Studies for the Molten Globule States of LBP, LIVBP, and RBP. Isothermal urea denaturation studies for the molten globule states of LBP, LIVBP, and RBP were carried out in CGH10 buffer containing 150 mM NaCl. Protein concentration was 10 μM. All of the samples were incubated for 5 h at 25 °C. This time was sufficient to attain equilibrium as monitored by the time dependence of the ellipticity. Longer incubation times did not result in any changes in the observed ellipticity. Denaturation was monitored using the CD signal at 222 nm for all proteins. The denaturant concentration was estimated by refractive index measurements.

Differential Scanning Calorimetry. Thermal denaturation for the molten globule states of all of the four proteins was carried out using a Microcal VP-DSC. DSC measurements were made for molten globules of 20 μM concentration as a function of ligand concentration ranging from 0−2 mM in CGH10 buffer. The protein solutions used for the DSC study

were dialyzed against double-distilled water. Buffers of the required pH and concentration were added to the dialyzed samples. The final pH of 3.4, 3.0, 3.0, and 3.2 was adjusted manually with 1 N HCl by using a pH meter for LBP, LIVBP, MBP, and RBP, respectively. In all cases, samples were incubated at 25 °C for 3 h at the required pH. This was followed by the addition of the ligand to the desired final concentration and incubation for an additional 30 min before the DSC scan. Ligands used for LBP, LIVBP, MBP, and RBP were L-leucine, L-isoleucine, D-(−)- maltose, and D-(+)- ribose, respectively. A scan rate of 90 °C/h was used for all four proteins. For all proteins, the reversibility of thermal unfolding was confirmed by carrying out a rescan. In all cases, at low pH, LBP, LIVBP, and RBP had reversibility greater than 90%. But, in the case of MBP, the reversibility was about 30%. DSC data was fit to a two-state unfolding with a baseline subtraction model using the Origin DSC software provided by Microcal Inc.

Estimation of ΔC_{pU} of Molten Globule Unfolding from Global Fits of the DSC Data. Global fits for the data for each protein in the presence of different concentrations of ligand were performed by determining excess heat capacity as a function of temperature using the experimentally determined values of ΔH for unfolding and T_m for free molten globules as well as ΔH for ligand binding and the association constant for molten globules at 25 °C as described previously by Jelesarov et al. (*47*) and are given below. The equation for fitting DSC data was derived by considering the following equilibria:

$$MG_f + L \overset{K_a}{\rightleftharpoons} MG_f - L \tag{1}$$

$$MG_f \overset{K_u}{\rightleftharpoons} MG_u \tag{2}$$

MG_f, L, and MG_u are the folded molten globule, ligand, and unfolded molten globule, respectively. The association constant K_a and equilibrium constant for unfolding K_u are expressed as follows:

$$K_a = \frac{[MG_f - L]}{[MG_f][L]} \tag{3}$$

$$K_u = \frac{[MG_u]}{[MG_f]} \tag{4}$$

The temperature dependence of K_a and K_u is given below:

$$K_a(T) = K_a(T_R) \times \exp\left[-\frac{\Delta H_a(T_R)}{R}\left(\frac{1}{T} - \frac{1}{T_R}\right) + \frac{\Delta C_{pB}}{R}\left(\ln\frac{T}{T_R} + \frac{T_R}{T} - 1\right)\right] \tag{5}$$

$$K_u(T) = \exp\left[-\frac{\Delta H_u(T_m)}{R}\left(\frac{1}{T} - \frac{1}{T_m}\right) + \frac{\Delta C_{pU}}{R}\left(\ln\frac{T}{T_m} + \frac{T_m}{T} - 1\right)\right] \tag{6}$$

where T_R and T_m are the reference temperatures for ligand binding and unfolding of molten globule, respectively. ΔC_{pB} and ΔC_{pU} are the specific heat capacity changes for ligand binding and unfolding, respectively. ΔH_a and ΔH_U are the enthalpies of ligand binding and unfolding, respectively. The values K_a and ΔH_a at T_R (25 °C) were determined by ITC studies. T_m and $\Delta H(T_m)$ are known from the thermal melt of the free molten globule. T_m is the temperature at which $K_u = 1$.

The enthalpy changes at different temperatures can be calculated as follows:

$$\Delta Ha(T) = \Lambda Ha(T_R) + \Delta C_{pB}(T - T_R) \tag{7}$$

$$\Delta H_u(T) = \Lambda H_u(T_m) + \Delta C_{pU}(T - T_m) \tag{8}$$

By considering the molten globule to have a single binding site for the ligand, we know by mass conservation that

$$[MG_{tot}] = [MG_f] + [MG_u] + [MG_f - L] = [MG_f] + K_u[MG_f] + K_a[MG_f][L] \tag{9}$$

Equations 3−9 give rise to the following expressions for determining concentrations of various species at any temperature T.

$$[MG_f] = \frac{[MG_{tot}]}{1 + K_u(T) + K_a(T)[L]} \tag{10}$$

$$[MG_u] = \frac{K_u(T)[MG_{tot}]}{1 + K_u(T) + K_a(T)[L]} \tag{11}$$

$$[MG_f - L] = \frac{K_u(T)[MG_{tot}][L]}{1 + K_u(T) + K_a(T)[L]} \tag{12}$$

$$[MG_f - L] = [L_{tot}] - [L] \tag{13}$$

where $[MG_{tot}]$, $[L_{tot}]$, $[L]$ are concentrations of the total molten globule, total ligand, and free ligand, respectively. Equations 12 and 13 are solved to derive an expression for $[L]$ in terms of K_u, K_a, $[L_{tot}]$, and $[MG_{tot}]$.

The enthalpy function is defined as follows:

$$\Delta H = \Delta H_u \frac{[MG_u]}{[MG_{tot}]} - \Delta H_a \frac{[MG_u] + [MG_f]}{[MG_{tot}]} \tag{14}$$

The heat capacity, $C_p(T)$ is determined by numerical differentiation of enthalpy with respect to temperature. The baseline-subtracted excess heat capacity change, ΔC_p, was derived by subtracting the contributions of MG_f, MG_u, and $MG_f - L$,

$$\Delta C_p = C_p(T) - \left[C_{pf}\frac{[MG_f]}{[MG_{tot}]} + (C_{pf} + \Delta C_{pU})\frac{[MG_u]}{[MG_{tot}]} + (C_{pf} + \Delta C_{pB})\frac{[MG_f - \mathrm{L}]}{[MG_{tot}]}\right] \tag{15}$$

where, C_{pf} is the heat capacity of the folded molten globule.

As can be seen from eqs 1−15, ΔCp is essentially a function of ΔC_{pB} and ΔC_{pU}. Hence, the specific heat capacity changes for binding and unfolding along with C_{pf} were allowed to vary for each of the molten globules to fit the DSC data obtained for molten globules in the presence of different ligand concentrations to eq 15.

Fluorescence Measurements. All measurements were carried out on a SPEX Fluoromax3 spectrofluorimeter using slit widths of 3 nm and 5 nm for excitation and emission,

respectively. Fluorescence measurements were made at different pH values of 1.0, 2.0, 3.0, 3.2, 3.4, 3.6, 3.8, 4.0, and 7.0. The protein concentrations used were 3−5 μM for LBP, LIVBP, and RBP and 0.5 μM for MBP. For obtaining the spectra of ligand-bound molten globules, protein samples were incubated at the required pH for 2 to 3 h at room temperature prior to ligand addition. Since all of the molten globules had a dissociation constant in the micromolar range, a ligand concentration 200-fold in excess of the protein was used to record the spectra of ligand-bound molten globules. After 30 min of incubation with ligand, samples were excited at 280 nm, and emission spectra were collected over the wavelength range of 300−400 nm. For the ANS binding study, the protein and ANS concentrations used were 1 and 100 μM, respectively. Samples were excited at 388 nm, and emission spectra were collected over the wavelength range of 420−550 nm. Each spectrum was an average of four consecutive scans. Buffer spectra were also taken under similar conditions and subtracted from the protein spectrum before analysis.

Isothermal Titration Calorimetry. All ITC measurements were carried out on a VP Isothermal Titration Calorimeter from MicroCal Inc. (Northampton, MA). Concentrations of 50 and 500 μM were used for protein and ligand, respectively, for all titrations. The ligands used for LBP, LIVBP, MBP, and RBP were L- Leu, L-Ile, D-(−)- maltose, and D-(+)- ribose, respectively. ITC measurements for ligand binding to molten globule states of LBP, LIVBP, MBP, and RBP were carried out at pH 3.4, 3.0, 3.0, and 3.2, respectively. To check for nonspecific binding, titrations of L-Ala, L-Ala, sucrose, and D-(+)-glucose were carried out against LBP, LIVBP, MBP, and RBP, respectively, at pH values corresponding to those of the native state and molten globule states. Ligand binding to the native state was measured at pH 8.0 for LBP and at pH 7 for LIVBP, MBP, and RBP. In all cases, protein and ligand solutions were separately incubated at 25 °C for 3 h and transferred to the cell and syringe, respectively. In all cases, the reference cell was filled with water. Once the cell temperature reached 25 °C and the baseline stabilized, 5 μL injections were performed at an interval of 4.2 min until saturation was observed. A stirring speed of 300 rpm was used for all measurements. The dilution of ligand into buffer and buffer into protein was carried out, and these dilution corrections were incorporated before data analysis. Data was analyzed by using the Origin Software package and fit to a single binding site in all cases (*48*).

ΔC_p of Ligand Binding and Isoelectric Point Calculations. The PDB IDs used were 1usk and 1usg for the ligand-bound and -free forms of LBP, 1z15 and 1z17 for the ligand-bound and -free forms of LIVBP, and 1anf and 1omp for the ligand-bound and -free forms of MBP (*43*, *49*−*51*). The ΔC_p of ligand binding to LBP, LIVBP, and MBP (ΔC_{pB}) was calculated from the change in nonpolar and polar accessible surface area (*ASA*) upon ligand binding. The following relationship between heat capacity and ΔASA (*52*) has been used for the calculation.

$$\Delta C_{pB} = (0.28 \pm 0.12)(\Delta ASA_{np}) - (0.09 \pm 0.3)(\Delta ASA_{pol})$$

ΔASA_{np} and ΔASA_{pol} are the changes in nonpolar and polar accessible surface area for ligand binding, respectively, which were calculated using the following relationship:

$$\Delta ASA = (ASA_P + ASA_L) - (ASA_{PL})$$

ASA_P, ASA_L, and ASA_{PL} are the accessible surface area for the protein, ligand, and protein−ligand complex, respectively. The *ASA* values were calculated from the free and ligand-bound structures of the native states of LBP, LIVBP, and MBP using NACCESS (*53*). The *ASA* for the free form of the ligands were calculated by using the ligand coordinates from the corresponding ligand-bound protein structure in the absence of protein.

The isoelectric point and charge of the protein were calculated using the protein calculator from http://www-.scripps.edu/∼cdputnam/protcalc.html.

Estimation of ΔC_{pU} of Molten Globule Unfolding from Individual DSC Scans. In the presence of ligand, the observed unfolding enthalpy for molten globule will have contributions from the denaturation of both ligand-free and ligand-bound forms of the molten globule. If *a* and *b* are the fractions of folded ligand-free and folded ligand-bound forms, respectively, then at any temperature *T*,

$$\Delta H_{obs} = a\Delta H_U(T) + b\Delta H_{U(MG-L)}(T) \qquad (16)$$

where $a + b = 1$, and ΔH_U and $\Delta H_{U(MG-L)}$ are the unfolding enthalpies of free and bound molten globules, respectively. *a* and *b* can be calculated from the value of $K_a(T)$. At the apparent T_m of thermal unfolding, approximately half of the total protein is folded, and half is unfolded. The calculation of $K_a(T)$ is described in the previous section. Since unfolding of the ligand-bound molten globule involves the dissociation of ligand,

$$\Delta Hu_{(MG-L)}(T) = -\Delta H_a(T) + \Delta H_U(T) \qquad (17)$$

Combining eqs 16 and 17,

$$\Delta H_{obs} = (a + b)\Delta H_{U(MG)}(T) - b\Delta H_a(T) \qquad (18)$$

$$\Delta H_U(T) = \Delta H_{obs} + b\,\Delta H_a(T) \qquad (19)$$

where $\Delta H_a(T)$ can be calculated from eq 7 using $T_R = 298$ K, and the values of $\Delta H_a(T_R)$ that were measured by ITC. Thus, the observed enthalpies of unfolding of molten globules in the presence of different ligand concentrations can be used for calculating enthalpies of the unfolding of ligand free molten globules at different temperatures. The linear dependence of the enthalpy of unfolding of the molten globule state on temperature was then used for determining the ΔC_{pU} values for molten globules.

RESULTS

LBP, LIVBP, and RBP Form Molten Globule States at Acidic pH. Spectroscopic characterization of the molten globule state of MBP has been previously reported by our group (*41*), and hence, is not discussed in this section. The data in Figure 1 show that LBP, LIVBP, and RBP also satisfy the criteria for the formation of a molten globule state at pH 3.4, 3.0, and 3.2, respectively, that is, native-like secondary structure, reduced tertiary structure, and exposed hydrophobic surface. The changes in secondary structure as a function of pH ranging from 1.0 to 7.0 for LBP, LIVBP, and RBP were

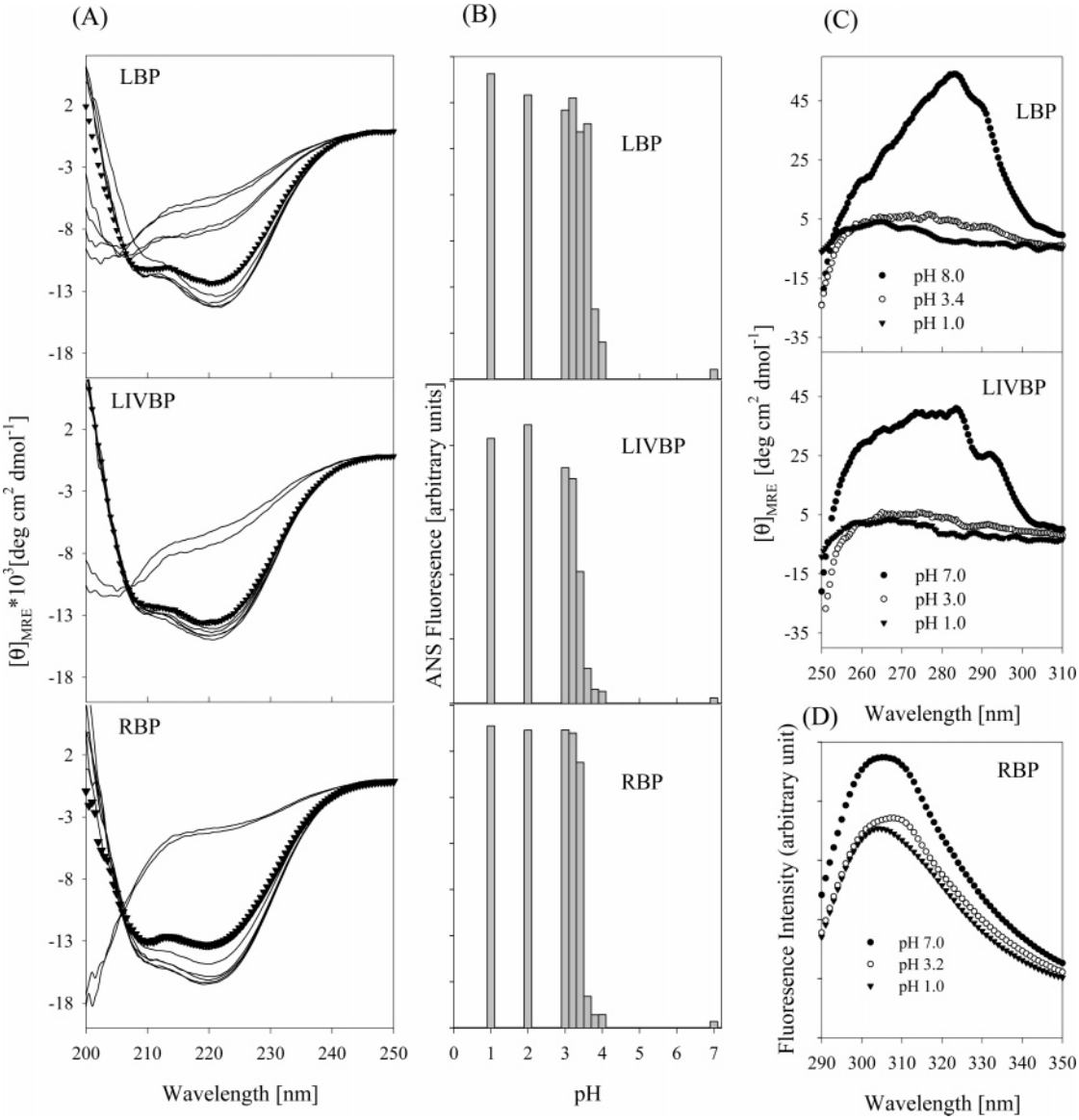

FIGURE 1: (A) Far-UV CD spectra for LBP, LIVBP, and RBP as a function of pH at 25 °C. The different pH values are 1.0, 2.0, 3.0, 3.2, 3.4, 3.6, 3.8, 4.0, and 7.0 (from top to bottom at 220 nm). Spectra for the molten globules are shown as filled triangles for all three proteins. (B) Fluorescence emission spectra of ANS in the presence of LBP, LIVBP, and RBP as a function of pH. The different pH values are similar to those used for far-UV CD measurements. ANS binding was monitored by the fluorescence emission intensity at 470 nm with excitation at 388 nm. (C) Near-UV CD spectra for LBP and LIVBP of native (pH 8.0 for LBP and pH 7.0 for LIVBP), molten globule (pH 3.4 for LBP and pH 3.0 for LIVBP), and acid unfolded states (pH 1.0 for LBP and LIVBP). (D) Fluorescence emission spectra with excitation at 280 nm of RBP for native (pH 7.0), molten globule (pH 3.2), and acid unfolded (pH 1.0) states. Similar data for MBP have been described previously (*41*, *45*). All of the spectra were recorded at 25 °C.

monitored by far-UV CD. The results are summarized in Figure 1A, which show that pH 3.4, 3.0, and 3.2 are the lowest pH values at which the far-UV CD spectra for LBP, LIVBP, and RBP, respectively, have been found to be similar (though not identical) to those of their native states (at neutral pH). Below the pH values of 3.4, 3.0, and 3.2, the far-UV CD spectra for LBP, LIVBP, and RBP, respectively, show a loss of secondary structure.

ANS binding to LBP, LIVBP, and RBP as a function of pH in the range of 1.0−7.0 was monitored by fluorescence spectroscopy. Significant binding of ANS to LBP, LIVBP, and RBP was observed at pH 3.4, 3.0, and 3.2, respectively (Figure 1B). ANS binding was not observed for any of these proteins at pH 4.0 and above.

Near-UV CD spectra have been acquired for LBP at pH 1.0, 3.4, and 8.0 and for LIVBP at pH 1.0, 3.0, and 7.0. The results are shown in Figure 1C. Near-UV CD spectra for LBP at pH 1.0 and pH 3.4 are very similar and show a large decrease in tertiary structure in comparison to the native state at pH 8.0. A similar observation was made for LIVBP at pH 1.0 and 3.0.

Since RBP has very weak ellipticity in the near-UV CD region owing to an absence of Trp residues, fluorescence spectra instead of near-UV CD spectra were acquired. The fluorescence spectra for RBP were acquired at pH values 1.0, 3.2, and 7.0. Figure 1D shows that the fluorescence spectra at pH 1.0 and 3.2 are very similar and are different from that of the native state at pH 7.0. The data in Figure 1 thus show that RBP also satisfied the criteria for a molten globule state at pH 3.2, that is, native-like secondary structure, reduced tertiary structure, and exposed hydrophobic surface.

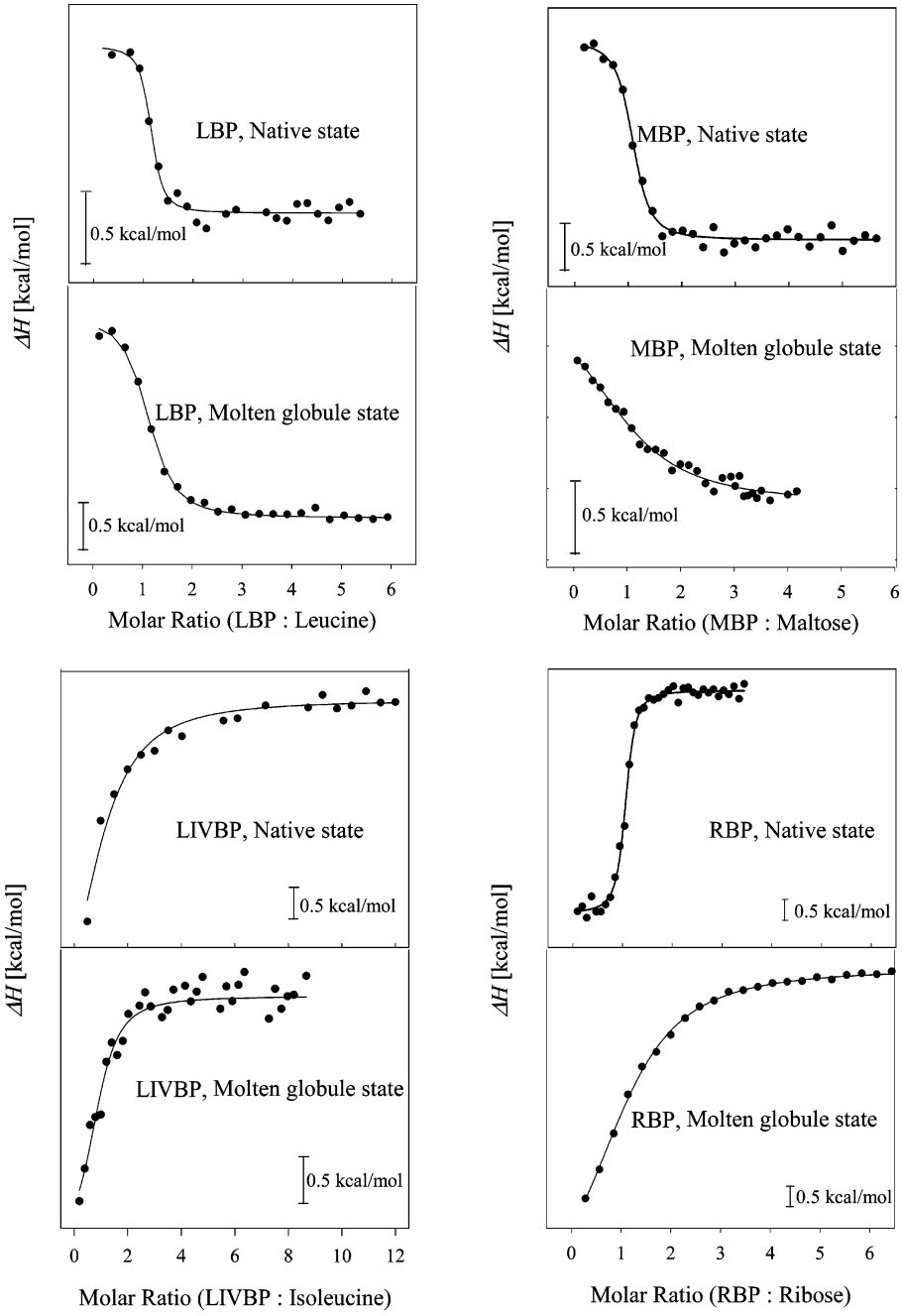

FIGURE 2: Profiles for the binding of native and molten globule states of LBP, LIVBP, MBP, and RBP with their respective ligands Leu, Ile, maltose, and ribose, respectively, at 25 °C, measured by ITC. Data points are shown as solid circles, and the fit is shown as a solid line.

The four proteins LBP, LIVBP, MBP, and RBP have calculated isoelectric points of 5.4, 5.5, 5.4, and 6.4, respectively, and at pH 3 have predicted net charges of 38.9, 38.9, 44.6, and 32.2, respectively.

Ligand Binding to the Native and Molten Globule States of LBP, LIVBP, MBP, and RBP. The ligand-binding affinity of the molten globule and the native states of LBP, LIVBP, MBP, and RBP was studied by isothermal titration calorimetry. Results are shown in Figure 2 and Table 1. It was observed that the molten globule state of LIVBP binds ligand with an affinity comparable to that of its native state, whereas those of LBP, MBP, and RBP bind ligand with affinities lower than those of their native states. In all of the experiments, heat of ligand dilution was very small in comparison to the heat of binding. After dilution correction, raw data were fitted assuming an identical and independent binding site model (*48*). The parameters K (binding constant), $\Delta H°$ (enthalpy of ligand binding), and n (number of binding sites) were obtained for the native and molten globule states of all four proteins. As expected, n was found to be close to one in all cases. $\Delta G°$ and $T\Delta S$ were calculated using the equations $\Delta G° = -RT \ln K$ and $T\Delta S = (\Delta H° - \Delta G°)$. The errors of the binding parameters listed in Table 1 are based on the standard errors obtained from repeated experiments at 25 °C. In the case of all four proteins, neither the native protein nor the corresponding molten globule, showed binding with non-cognate ligands (Supporting Information, Figure 4).

Spectroscopic Characterization of Ligand-Bound Molten Globule States. The change in tertiary structure for the molten globules of all four proteins on ligand binding has been monitored by Trp and ANS fluorescence as well

Table 1: Thermodynamic Parameters for Ligand Binding at 25 °C Obtained from ITC Studies of Native (N) and Molten Globule (MG) States of Periplasmic Binding Proteins[a]

	$K_A \times 10^{-5}$ (M^{-1})		$\Delta H_A°$ (kcal/mol)		$T\Delta S$ (kcal/mol)		$\Delta G°$ (kcal/mol)	
protein/ligand	N	MG	N	MG	N	MG	N	MG
LBP/Leu	8.3 ± 2.8	1.9 ± 0.6	1.2 ± 0.1	2.2 ± 0.1	−9.1 ± 0.4	−9.3 ± 0.4	−8.0 ± 0.3	−7.2 ± 0.3
LIVBP/Ile	1.7 ± 0.6	1.5 ± 0.1	−7.1 ± 0.4	−2.8 ± 0.1	0.1 ± 0.7	−4.2 ± 0.1	−7.0 ± 0.4	−7.0 ± 0.1
MBP/maltose	7.8 ± 2.0	0.3 ± 0.1	2.3 ± 0.1	1.6 ± 0.1	−10.2 ± 0.1	−7.5 ± 0.2	−7.9 ± 0.2	−6.0 ± 0.3
RBP/ribose	25.9 ± 3.0	0.8 ± 0.0	−4.6 ± 0.4	−10 ± 1.1	−4.0 ± 0.2	3.4 ± 1.1	−8.7 ± 0.1	−6.6 ± 0.1

[a] The pH values were 8.0 for LBP and 7.0 for LIVBP, MBP, and RBP in the native states and pH 3.4, 3.0, 3.0 and 3.2 for LBP, LIVBP, MBP, and RBP, respectively, in molten globule states. The error estimate was derived from the standard error of repeated experiments under similar conditions.

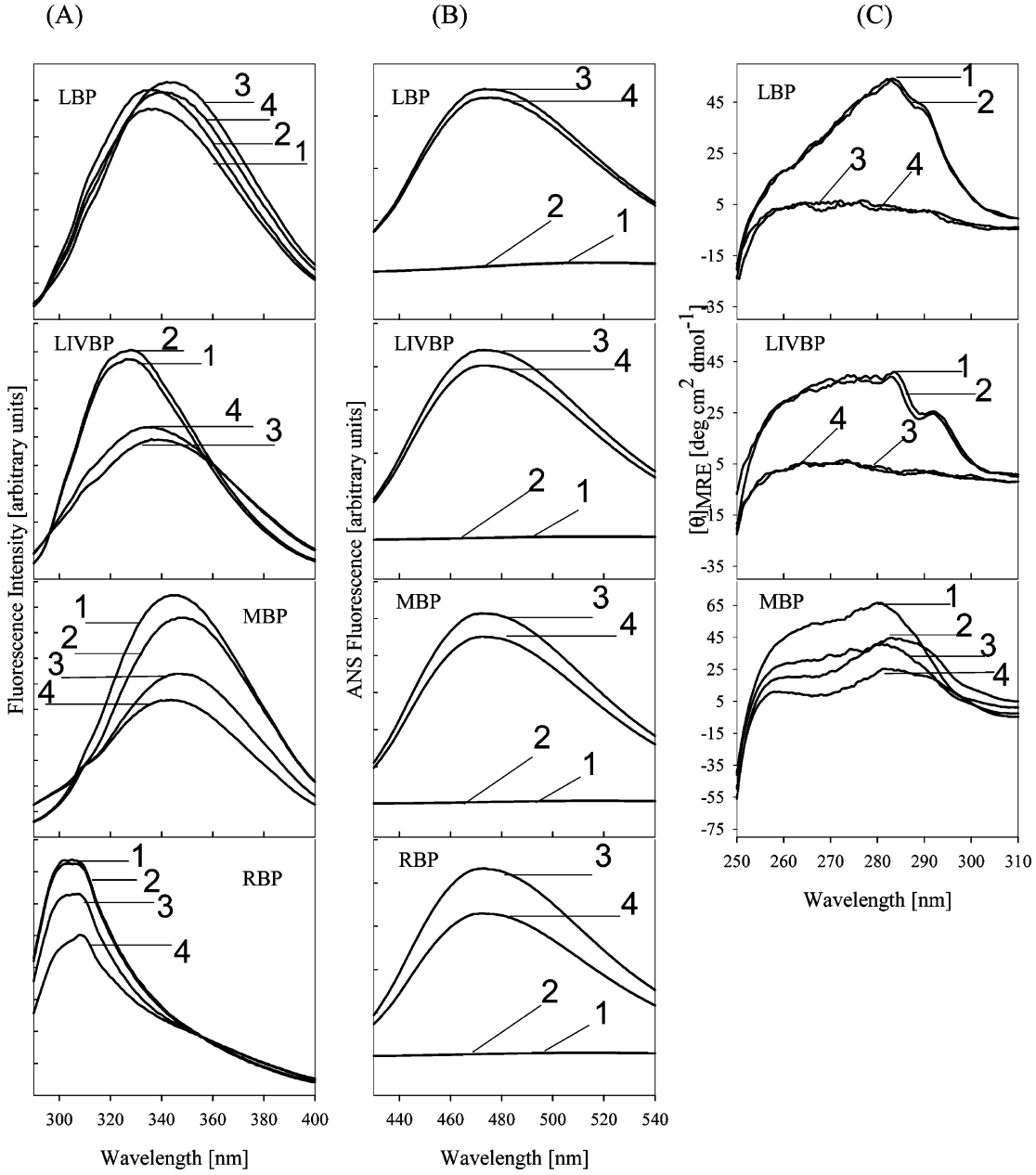

FIGURE 3: Fluorescence and CD spectra for ligand-bound and free forms of native and molten globule states of periplasmic binding proteins at 25 °C. (A) Intrinsic fluorescence emission spectra with excitation at 280 nm. (B) ANS fluorescence spectra with excitation at 388 nm. (C) Near-UV CD spectra. In all of the panels, curves 1, 2, 3, and 4 represent the native state, ligand-bound native state, molten globule state, and ligand-bound molten globule state, respectively.

as by near-UV CD. Figure 3A shows that Trp fluorescence spectra for the ligand-bound and -free forms of the molten globule states are very similar to each other but are different from the corresponding native states for LBP and LIVBP. For MBP, ligand binding to the molten globule results in a small red shift, whereas for RBP, there is an increase in fluorescence intensity. However, in both cases, the fluorescence of the ligand-bound molten

Table 2: Thermodynamic Unfolding Parameters for the Molten Globule and Native States of Periplasmic Binding Proteins, Obtained from DSC Studies[a]

	MG		N		MG − N
protein	T_m (°C)	$\Delta H°(T_m)$ (kcal/mol)	T_m (°C)	$\Delta H°(T_m)$ (kcal/mol)	ΔT_m (°C)
LBP	35.4	71	60.7	128	−25.3
LBP, Leu	47.0	105	67.8	166	−20.8
LIVBP	43.1	110	67.0	163	−23.9
LIVBP, Ile	50.4	132	74.6	218	−24.2
MBP	46.0	121	63.3	205	−17.3
MBP, maltose	56.4	142	75.3	225	−18.9
RBP	37.6	65	62.6	111	−25.0
RBP, ribose	48.4	82	75.4	132	−27.0

[a] DSC studies were carried out in the presence (of 1 mM of the respective ligand) and in the absence of ligand for both native and molten globule states. The average errors in T_m and $\Delta H°(T_m)$ are ± 0.2 °C and 20%, respectively, as determined from repeat experiments.

globule state is different from that of the ligand-bound native state.

ANS binding for the ligand-bound and -free forms of the molten globule states was observed to be similar for all four proteins, although the RBP molten globule shows slightly decreased ANS binding in the presence of ligand (Figure 3B). As mentioned above, ANS binds only to the molten globule state and not to the native state. The data therefore clearly demonstrate that ligand binding to the molten globule does not result in conversion to the native state for any of the four proteins examined.

Near-UV CD spectra for three of the proteins in the presence and absence of ligand are shown in Figure 3C. As described previously, RBP lacks Trp residues, and therefore, the molten globule of RBP could not be characterized using this technique. For LBP and LIVBP, ligand binding does not result in any change in the near-UV CD spectrum, for neither the native (curves 1 and 2) nor the molten globule (curves 3 and 4) states. In the case of MBP, addition of the ligand results in a decrease in the near-UV CD signal for the native state and an increase for the molten globule state. There are 8 Trp and 15 Tyr residues in MBP, and the observed changes in near-UV CD spectra could probably be due to a change in the relative orientations of one or more of the Trp and Tyr residues in MBP upon ligand binding. A Trp residue and a Tyr residue are in close proximity to the ligand binding site, and these are likely to be the major contributors to the change in the near-UV CD signal on ligand binding.

The data in Figure 3 show that ligand binding to the molten globules of LBP and LIVBP does not result in any substantial ordering of the molecule. For MBP and RBP molten globules, ligand binding may be coupled to some degree of structure formation. However, even for these two proteins, the ligand-bound molten globule is distinct from the ligand-bound native state because the former binds ANS and has an intrinsic fluorescence spectrum different from that of the latter (Figure 3A and B).

Thermodynamic Stability for Molten Globule States. Stabilities of the molten globule states for all four proteins were characterized by thermal and isothermal chemical denaturation. A urea denaturation study for the molten globule state of MBP was reported previously (*41*). Using

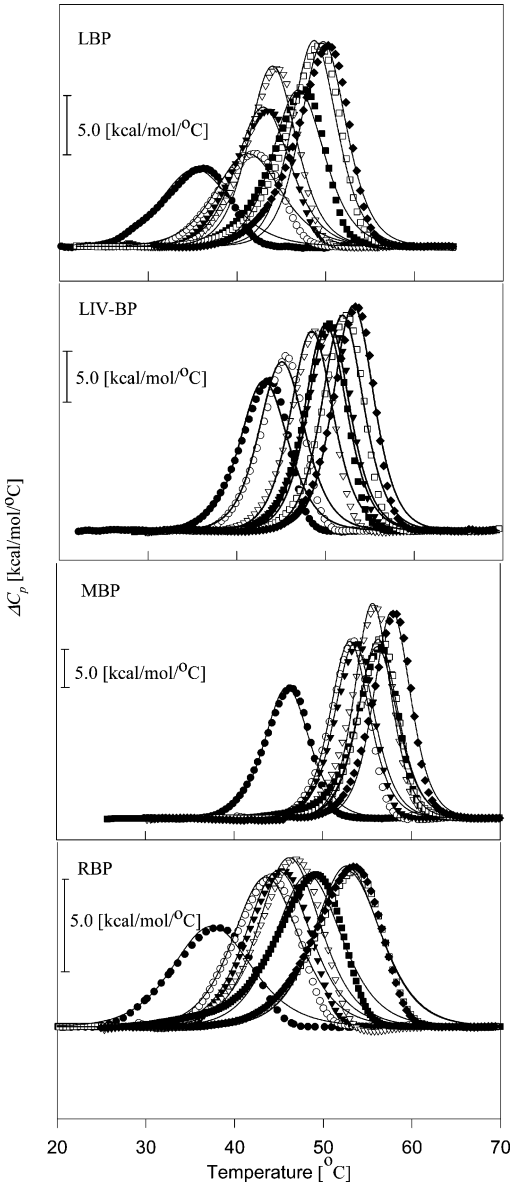

FIGURE 4: Baseline subtracted DSC scans for the free and ligand-bound forms of the molten globule states of periplasmic binding proteins. Leu, Ile, maltose, and ribose are used as the ligands for LBP, LIVBP, MBP, and RBP, respectively. Data points at different ligand concentrations are shown with the following symbols: ● (0.0 mM), ○ (0.05 mM), ▼ (0.1 mM), ▽ (0.5 mM), ■ (1.0 mM), □ (1.5 mM), and ◆ (2.0 mM), and two state fits to the data are shown as thin solid lines. Protein concentration was 0.3−0.5 mg/mL in all cases.

the same method, isothermal chemical denaturation for molten globule states of LBP, LIVBP, and RBP was carried out at 25 °C with urea. However, the reduced stability of the molten globule states resulted in a lack of a significant native baseline, and the data, therefore, could not be analyzed (data not shown). Unfolding thermodynamics for the molten globule states for all four proteins were, therefore, characterized using differential scanning calorimetry. Thermal unfolding for the molten globule states of LBP, LIVBP, and RBP was found to have a reversibility of about 90%. However, in the case of MBP, the reversibility was only about 30%. DSC studies were carried out in the presence and absence of the respective ligand for both molten globule states and native states for all four proteins. The results are shown in Figure 1 (Supporting Information) and Table 2. Molten

Table 3: Estimated Heat Capacities of Unfolding (ΔC_{pU}) and Ligand Binding (ΔC_{pB}) for Periplasmic Binding Proteins

	ΔC_{pu} (kcal/mol/°C)					ΔC_{pB} (kcal/mol/°C)	
protein	MG[a]	MG[b]	N[c]	(ΔC_{pu}(MG)/ ΔC_{pu}(N)) × 100		N	MG[d]
LBP	4.1 ± 0.6	3.1 ± 0.1	6.1 ± 0.6	67.1[e]	50.8[f]	0.17[g]	−0.12 ± .03
LIVBP	3.2 ± 0.2	1.8 ± 0.2	5.6 ± 0.6	56.4[e]	32.1[f]	0.22[g]	−0.04 ± .03
MBP	3.3 ± 0.7	3.2 ± 0.3	5.4 ± 1.9	61.5[e]	59.2[f]	0.14[g]	1.20 ± .04
RBP	1.2 ± 0.3	1.3 ± 0.1	4.5 ± 0.2	27.7[e]	28.9[f]	0.4[h]	0.44 ± .03

[a] Estimated from the linear dependence of the enthalpy of molten globule unfolding on temperature derived from individual fits of DSC scans as a function of ligand concentration. [b] Derived by global fitting of DSC data obtained for molten globule unfolding as a function of ligand concentration. [c] Estimated from the linear dependence of $\Delta H°(T_m)$ on T_m (*42*) for data in Table 1 (Supporting Information). [d] Derived by global fitting of DSC data obtained for molten globule unfolding as a function of ligand concentration. [e] Calculated from MG[a] and N[c]. [f] Calculated from MG[b] and N[c]. [g] Calculated ΔC_{pB} for ligand binding to the native state estimated as described in ref *52* (see text for details). [h] ΔC_{pB} for RBP could not be calculated because no structure of the ligand bound form is available. The measured values ΔC_{pB} for L-arabinose and D-galactose binding to L-arabinose binding protein were approximately 0.4 kcal/mol/°C (*54*), and therefore, this value was assumed for RBP.

Table 4: Unfolding Parameters for the Molten Globule States of Periplasmic Binding Proteins as a Function of Ligand Concentration Derived from Individual DSC Fits[a]

	LBP		LIVBP		MBP		RBP	
ligand (mM)	T_m (°C)	$\Delta H°(T_m)$ (kcal/mol)	T_m (°C)	$\Delta H°(T_m)$ (kcal/mol)	T_m (°C)	$\Delta H°(T_m)$ (kcal/mol)	T_m (°C)	$\Delta H°(T_m)$ (kcal/mol)
0.0	35.4	71	43.1	110	46.0	121	37.6	65
0.05	41.3	80	45.1	117	53.0	143	43.6	80
0.1	43.0	98	48.5	129	53.6	143	45.0	83
0.5	44.0	112	50.0	132	55.6	159	46.2	86
1.0	47.0	105	50.4	132	56.4	142	48.4	82
1.5	48.7	121	52.0	135	56.2	146	52.8	84
2.0	49.8	121	53.0	139	57.8	157	52.7	85

[a] Average errors in T_m and $\Delta H°(T_m)$ are ± 0.2 °C and 5%, respectively, as determined from repeat experiments.

globule thermal melts were also carried out as a function of ligand concentration (Figure 4). All DSC data were fitted with a baseline-subtracted two-state unfolding model. As expected, unfolding thermodynamic parameters for molten globule states for all four proteins show a large destabilization in comparison to those of their respective native states. Furthermore, with increasing ligand concentration, the thermal stability of molten globule increases, indicating an increase in the proportion of ligand-bound molten globule.

ΔC_p of Ligand Binding to the Native States. ΔC_{pB} values for ligand binding to the native states of LBP, LIVBP, and MBP were calculated as described in Materials and Methods and are listed in Table 3.

ΔC_{pB} for ligand binding to RBP could not be calculated because the ligand-bound structure of RBP was unavailable. However, ΔC_{pB} values for L-arabinose and D-galactose binding to L-arabinose binding proteins were ~0.4 kcal/mol/°C as reported previously (*54*). Since ribose is also a monosaccharide similar in size to galactose, the same value was assumed to hold for RBP. This ΔC_{pB} value was similar to our calculated values of ΔC_{pB} for ligand binding to LBP, LIVBP, and MBP. We assume that ΔC_{pB} for ligand binding to the molten globule states of the periplasmic binding proteins will be quite similar to corresponding ΔC_{pB} values for ligand binding to the native states. This is based on the following arguments. First, it is unlikely that ligand binding in the molten globule buries a larger ligand surface than that in binding to the native state. The spectroscopic data suggest that there do not appear to be large changes in exposed hydrophobic surfaces or the tertiary structure of protein upon ligand binding to the molten globule. Hence, in the absence of large protein conformational changes upon binding, the magnitude of ΔC_{pB} for ligand binding to the molten globule will be less than the corresponding value for the native state. Second, the enthalpies of binding measured by ITC are also small, with the exception of RBP (Table 1). Also, as will be seen from the analysis below, the precise value of ΔC_{pB} is not important because all ΔC_{pB} values are considerably smaller than the corresponding ΔC_p values of unfolding of the molten globules.

ΔC_p for Unfolding of Molten Globule States Estimated from an Analysis of Individual DSC Scans. The DSC data for the molten globule states of all four proteins, carried out as a function of cognate ligand concentration, were subjected to individual two-state fits. The results are shown in Table 4 and Figure 4. All DSC data have been fitted with a baseline-subtracted two-state model. Molten globule states for all four proteins show an increase in T_m with increasing concentration of their respective ligand. The $\Delta H°(T_m)$ values obtained from DSC studies listed in Table 4 contain contributions from ligand-binding enthalpy in addition to unfolding and result from the unfolding transitions of both ligand-free and -bound proteins. The measured enthalpies were corrected for these effects as described in the Materials and Methods section. The enthalpy of unfolding of the molten globule state at each T_m value (Table 4) was calculated as described in Materials and Methods, and the values are listed in Table 5. Values of $K_a(T_R)$, $\Delta H_A(T_R)$, and ΔC_{pB} were taken from Tables 1 and 3. ΔC_{pU} values for all four molten globules states were estimated from the linear dependence of the enthalpy of unfolding of the molten globule state on temperature (enthalpy data in Table 5 and Figure 2 (Supporting Information)). The values of ΔC_{pU} for

Table 5: Calculated Enthalpy for Unfolding of the Molten Globule State as a Function of Temperature[a]

	LBP		LIVBP		MBP		RBP	
ligand (mM)	T (°C)	$\Delta H_U(T)$ (kcal/mol)	T (°C)	$\Delta H_U(T)$ (kcal/mol)	T (°C)	$\Delta H_U(T)$ (kcal/mol)	T (°C)	$\Delta H_U(T)$ (kcal/mol)
0.0	35.4	71.0	43.1	110.0	46.0	121.0	37.6	65.0
0.05	41.3	84.5	45.1	118.4	53.0	146.8	43.6	80.8
0.1	43.0	103.0	48.5	131.2	53.6	147.6	45.0	84.1
0.5	44.0	117.4	50.0	134.7	55.6	164.7	46.2	88.1
1.0	47.0	110.9	50.4	134.8	56.4	147.9	48.4	84.5
1.5	48.7	127.2	52.0	138.1	56.2	151.9	52.8	86.4
2.0	49.8	127.4	53.0	142.3	57.8	163.1	52.7	88.1

[a]See text for details.

all fourmolten globule states calculated in the above manner are listed in Table 3, column 2.

ΔC_p values for unfolding of the native states for LIVBP, MBP, and RBP were reported previously (*42*). The ΔC_p values were derived by measuring $\Delta H°(T_m)$ and T_m as a function of pH in the pH range 6.5−9.5. In the case of LBP, thermal denauration at pH values below 8.0 was found to be non-two state, whereas at pH 8.0, it is two state. Hence for LBP, DSC was carried out as a function of urea concentration from 0.2 to 2 M with an interval of 0.2 M at pH 8. LBP showed a decrease in T_m with increasing concentrations of urea. The results are shown in Supporting Information (Table 1 and Figure 3). The value of ΔC_p for the unfolding of LBP has been estimated from the slope of the linear dependence of ΔH_U (T_m) upon T_m and as expected is quite similar to the corresponding value for its close homologue LIVBP. We recently used a similar approach to measure the ΔC_p for unfolding of the homodimeric *E. coli* toxin CcdB (*55*). ΔC_p for unfolding of the native states for all four proteins are also shown in Table 3.

ΔC_p for the Unfolding of Molten Globule States Estimated from Global Fits of DSC Scans. The data obtained for each of the molten globules in the presence of different amounts of ligand was also subjected to a global fit as described in Materials and Methods to obtain estimates for ΔC_{pU} and ΔC_{pB}. (Table 3 and Figure 5). These fits were made with the assumptions that ligand binding and unfolding are both two state and that the ΔC_p values for ligand binding and unfolding are temperature-independent. The quality of the global fits is much worse than those of the individual two states, presumably because of the smaller number of adjustable parameters. However, the values of ΔC_{pU} obtained were similar with both fitting procedures, and the magnitude of ΔC_{pB} was signficantly less than that of ΔC_{pU} in all cases. The poor global fits might also result from the presence of intermediates in the thermal unfolding, temperature dependence of the ΔC_p values, and problems with baseline fitting. Despite these caveats, the DSC data clearly demonstrate that the molten globules of all four proteins bind ligand and show distinct thermal transitions with appreciable positive changes in heat capacity upon thermal unfolding.

DISCUSSION

We have shown that all four periplasmic binding proteins (LBP, LIVBP, MBP, and RBP) form molten globule states at acidic pH values ranging from 3 to 3.4. The molten globule states of these proteins exhibit a marked amount of secondary structure, which from the far-UV CD spectra appear to be similar to that of the native state with respect to the amount and type of secondary structure. They also show a loss of tertiary structure and an increase in the hydrophobic surface accessible to the solvent. These characteristics are similar to those of previously reported molten globules for other proteins (*8*, *56*−*60*). A decrease in pH leads to the protonation of negatively charged residues of the protein and a consequent increase in the total positive charge of the protein. This results in increased electrostatic repulsion on the surface of the protein. Consequently, there is a loss of tertiary structure and some hydrophobic residues that were formerly in the interior of the protein become more exposed to the solvent than those in the native state. This results in a reduced near-UV CD signal and binding of the hydrophobic dye ANS. All four proteins, which have been used in this study, satisfied the above criteria typically used to define the molten globule state (Figure 1). However, it must be noted that the decrease in the near-UV CD signal need not imply a loss of tertiary structure. Thermal denaturation studies show that as expected the molten globule states of all four proteins show a large decrease in T_m in comparison to that of the native state.

Thermodynamics associated with unfolding of molten globule states have been measured previously. However, different results have been obtained for different proteins and in some cases for the same protein by different groups. Thermal unfolding of the molten globule state of apo α-lactalbumin at acidic pH is observed to be accompanied by small or zero values of ΔH and ΔC_p (*35*−*39*). However, other calorimetric measurements (*61*) revealed a significant negative heat capacity difference between the molten globule and unfolded states. The same study reported a negative enthalpy of unfolding of the molten globule. An earlier calorimetric study (*62*) of the unfolding of the molten globule of the same protein in the presence of GdmCl at neutral pH reported a ΔC_p of unfolding that was about 80% of the value for unfolding from the native state. Spectroscopic studies of the denaturation of molten globule states of MBP and Yeast iso-1-cyt-*c* proteins showed ΔC_{pU} values of that were 70% and 60%, respectively, of the corresponding values for the native states (*40*, *41*, *63*−*65*), indicating that there is a considerable burial of nonpolar surfaces in these molten globules. Another spectroscopic study of the denaturation of bovine and horse cytochromes-*c* by $LiCl/CaCl_2$ (*66*) or thermal unfolding at low pH (*67*) yielded ΔC_{pU} values for the molten globule that were about 30% of those of the native state. A recent study of a salt-stabilized alkaline molten globule of the same protein yielded a value of ΔC_{pU} that

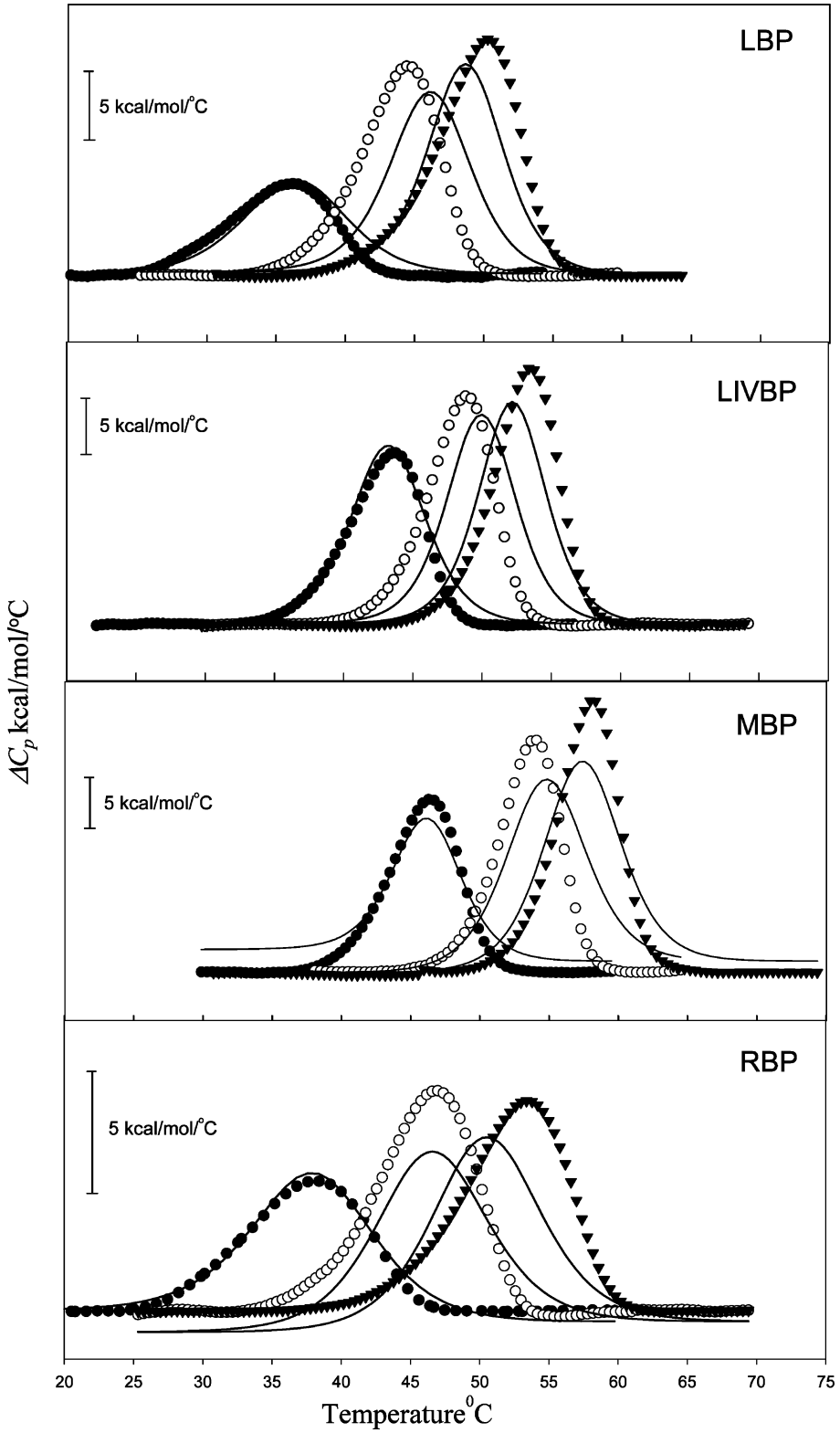

FIGURE 5: Global fits of baseline subtracted DSC data for representative DSC scans of the free and ligand-bound forms of the molten globule states of LBP, LIVBP, MBP, and RBP. Data points at different ligand concentrations are shown with the following symbols: ● (0.0 mM), ○ (0.5 mM), and ▼ (2 mM). Global fits to the data are shown as thin solid lines.

was about 50% of that of the native state. The values of $\Delta H°(T_m)$, T_m, and ΔC_{pU} for the unfolding of native and molten globule states in the present study are summarized in Tables 2 and 3. These molten globule states show 28−67% of the ΔC_{pu} of their native states and have positive enthalpies of unfolding. The cooperativity of folding, which is a feature of globular proteins, is thought to result from the tight and unique packing of amino acid residues. In the absence or reduction of tertiary structure, it has been asserted that one cannot observe cooperativity between all the elements of proteins (*68*). The enthalpy change associated with protein thermal unfolding is thought to consist primarily of contributions arising from the solvent exposure of buried nonpolar groups in the protein as well as the rupture of the

secondary and tertiary structure hydrogen bonds (*68*). The heat-capacity changes associated with the unfolding of proteins contain a large positive contribution due to the exposure of previously buried hydrophobic residues to water and a smaller negative contribution associated with the rupture of hydrogen bonds (*69*, *70*).

There have been relatively few calorimetric characterizations of molten globule states, especially in the absence of denaturants. This is presumably because of the low/negative enthalpies of unfolding of some molten globules. In addition, molten globules show a tendency to aggregate because of the exposed hydrophobic surface, and this may result in irreversible thermal unfolding. Recent isothermal titration studies have monitored molten globule transitions in cyt-*c* induced by either salt (*71*) or acid (*72*). ΔC_{pU} for the native to molten globule transition was found to have values about 20% of that for ΔC_{pU} of unfolding of the native state, again suggesting that the molten globule of cyt-*c* retained significant structure. A similar study of the molten globule of sperm whale apomyoglobin reported an undetectable enthalpy of unfolding (*73*).

Although molten globules show little or no tertiary structure as assessed by near-UV CD, the role of specific interactions in stabilizing molten globules remains unclear. The extent of specific packing in molten globules of α-lactalbumin, cyt-*c*, apomyoglobin, and staphylococcal nuclease has previously been studied by examining the effect of point mutations on the stabilities of native and molten globule states. These results indicate a small but significant degree of specific native-like packing interactions in these molten globules (*74*). In the present studies, the relatively high heat capacity, unfolding enthalpies, and ligand-binding affinity of the molten globules are all consistent with an appreciable degree of ordering. The ligand binding in these proteins involves several residues, which are spatially distant in the three-dimensional structure. Hence, it appears reasonable to assume that ligand binding to the molten globule is only possible if there is a native state-like topology and not just a localized structural organization. However, further structural studies are needed to confirm this assertion. The picture that emerges from thermodynamic parameters of molten globule states of the four proteins is that the molten globule state contains almost all of the secondary structure and some tertiary structure, which has been observed in molten globule states of some other proteins (*40*, *75*). The binding of ligand to the molten globule shows that even though the molten globule state appears to lose tertiary structure relative to the native state as assayed by near-UV CD the binding pocket is retained in a native-like conformation, and hence, an appreciable degree of specific packing is likely to be present in these molten globules.

Binding is not as sensitive an assay for the detection of small amounts of correctly folded protein as enzymatic activity. A recent study by Gebhard et al. elegantly demonstrates the advantages of using enzymatic activity to detect small populations of folded molecules (*76*). Nevertheless, for proteins that lack enzymatic activity, specific ligand binding is also a useful probe for correct folding. The data also demonstrate that the lack of an observable near-UV CD signal does not necessarily imply a lack of specific packing and/or a substantial loss of protein tertiary structure. It may, therefore, be worth re-examining the extent of tertiary structure in other previously characterized molten globules by appropriate functional and spectroscopic assays. In the majority of previous characterizations, no functional/ligand binding assays have been carried out. Ligand-binding affinity is a sensitive probe of tertiary structure; however, care must be taken to demonstrate that ligand binding does not induce tertiary structure in the molten globule being studied. All four proteins do not have prosthetic groups; therefore, it is likely that these molten globule states are stabilized by hydrophobic interactions, specific packing, and hydrogen bonding.

The ligand binding affinity of both native and molten globule states was similar similar for LIVBP. In the case of LBP, the affinity of the molten globule for ligand is only 4-fold lower than that of the native state (Table 1). Interestingly, LBP and LIVBP both bind amino acids with hydrophobic side chains. For MBP and RBP, which bind carbohydrate ligands, the molten globule bound with about 30-fold lower affinity than the native state. This might be because binding to carbohydrate is mediated by several hydrogen bonds that require an ordered binding pocket, whereas binding to the amino acid is mediated by a less specific van der Waals interaction with the side chain, although the amino and carboxyl groups of the amino acid are involved in specific hydrogen bonds with the protein (*43*, *51*, *77*).

Most of the earlier studies on molten globules have focused on relatively small proteins. There have been fewer studies on the folding of large multidomain proteins because of aggregation and lack of reversibility. In contrast, all of the four large periplasmic binding proteins examined in the present study show reversible folding. LBP and LIVBP are closely related with a sequence identity of 77%, whereas MBP and RBP are sequentially unrelated to each other and to LBP/LIVBP. However, all four proteins adopt similar three-dimensional structures. Three of these proteins (LBP, LIVBP, and RBP) belong to the same SCOP family (L-arabinose binding proteins) and fold (periplasmic binding protein, I). MBP belongs to a different family (phosphate binding protein) and to a similar fold (periplasmic binding protein, II) (*78*, *79*). The observation that these sequentially unrelated but structurally similar proteins all form molten globules at low pH suggests that this may be an intrinsic feature of the periplasmic binding protein folds. As a consequence of their large size, all four proteins are predicted to have significant positive charge (+30 to +45) at pH 3.0. All of these proteins undergo translocation across the inner membrane of *E. coli*, and interestingly, all form molten globules *in vitro*. Since molten globules have previously been implicated in protein translocation, the present studies have biological relevance. In the case of MBP and pre-MBP, a collapsed, molten globule-like intermediate has been shown to form within a few milliseconds of denaturant dilution (*80*). This intermediate is competent to bind the chaperone SecB. Future studies will investigate whether similar kinetic intermediates are formed during the refolding of the other three periplasmic proteins. There are a total of 42 annotated periplasmic binding proteins in the *E. coli* K12 genome ranging in size from 185 to 566 amino acids. These have average predicted charges of 44 ± 13 at pH 3.0. All periplasmic binding proteins for which crystal structures are currently available adopt a characteristic two-domain struc-

ture with a cleft for ligand binding. It will be interesting to examine whether other members of this important family also form similar ordered molten globule states at low pH and whether these play any role either in the translocation process or during periplasmic folding.

ACKNOWLEDGMENT

LBP/LIVBP and RBP expression plasmids were kindly provided by Dr. L. Luck and S. Mowbray, respectively. We thank the reviewers for helpful suggestions.

SUPPORTING INFORMATION AVAILABLE

Thermodynamic parameters for the thermal unfolding of LBP at pH 8.0; DSC scans for the free and ligand-bound forms of the molten globule and native states for LBP, LIVBP, MBP, and RBP; ΔC_{pU} estimation for the unfolding of molten globules of all four periplasmic binding proteins and the native state of LBP; and ITC profiles for the interaction of LBP molten globule with Ala and Leu. This material is available free of charge via the Internet at http://pubs.acs.org.

REFERENCES

1. Ptitsyn, O. B. (1995) How the molten globule became, *Trends Biochem. Sci. 20*, 376−379.
2. Ptitsyn, O. B. (1973) Stages in the mechanism of self-organization of protein molecules, *Dokl. Akad. Nauk SSSR 210*, 1213−1215.
3. Wong, K. P., and Tanford, C. (1973) Denaturation of bovine carbonic anhydrase B by guanidine hydrochloride. A process involving separable sequential conformational transitions, *J. Biol. Chem. 248*, 8518−8523.
4. Dolgikh, D. A., Gilmanshin, R. I., Brazhnikov, E. V., Bychkova, V. E., Semisotnov, G. V., Venyaminov, S., and Ptitsyn, O. B. (1981) Alpha-Lactalbumin: compact state with fluctuating tertiary structure? *FEBS Lett. 136*, 311−315.
5. Wong, K. P., and Hamlin, L. M. (1974) Acid denaturation of bovine carbonic anhydrase B, *Biochemistry 13*, 2678−2683.
6. Prost, J., and Rondelez, F. (1991) Structures in colloidal physical chemistry, *Nature 350*, 11−23.
7. Dolgikh, D. A., Kolomiets, A. P., Bolotina, I. A., and Ptitsyn, O. B. (1984) 'Molten-globule' state accumulates in carbonic anhydrase folding, *FEBS Lett. 165*, 88−92.
8. Ohgushi, M., and Wada, A. (1983) 'Molten-globule state': a compact form of globular proteins with mobile side-chains, *FEBS Lett. 164*, 21−24.
9. Dobson, C. M. (1994) Protein folding. Solid evidence for molten globules, *Curr. Biol. 4*, 636−640.
10. Ewbank, J. J., Creighton, T. E., Hayer-Hartl, M. K., and Ulrich, Hartl, F. (1995) What is the molten globule? *Nat. Struct. Biol. 2*, 10−11.
11. Kuwajima, K. (1989) The molten globule state as a clue for understanding the folding and cooperativity of globular-protein structure, *Proteins 6*, 87−103.
12. Pande, V. S., and Rokhsar, D. S. (1998) Is the molten globule a third phase of proteins? *Proc. Natl. Acad. Sci. U.S.A. 95*, 1490−1494.
13. Ermacora, M. R., Ledman, D. W., and Fox, R. O. (1996) Mapping the structure of a non-native state of staphylococcal nuclease, *Nat. Struct. Biol. 3*, 59−66.
14. Shortle, D., and Ackerman, M. S. (2001) Persistence of native-like topology in a denatured protein in 8 M urea, *Science 293*, 487−489.
15. Bychkova, V. E., and Ptitsyn, O. B. (1993) The molten globule in vitro and in vivo, *Chemtracts: Biochem. Mol. Biol. 4*, 133−163.
16. Zhou, B., Tian, K., and Jing, G. (2000) An in vitro peptide folding model suggests the presence of the molten globule state during nascent peptide folding, *Protein Eng. 13*, 35−39.
17. Bychkova, V. E., and Ptitsyn, O. B. (1995) Folding intermediates are involved in genetic diseases? *FEBS Lett. 359*, 6−8.
18. Denning, G. M., Anderson, M. P., Amara, J. F., Marshall, J., Smith, A. E., and Welsh, M. J. (1992) Processing of mutant cystic fibrosis transmembrane conductance regulator is temperature-sensitive, *Nature 358*, 761−764.
19. Thomas, P. J., Shenbagamurthi, P., Sondek, J., Hullihen, J. M., and Pedersen, P. L. (1992) The cystic fibrosis transmembrane conductance regulator. Effects of the most common cystic fibrosis-causing mutation on the secondary structure and stability of a synthetic peptide, *J. Biol. Chem. 267*, 5727−5730.
20. Yang, Y., Janich, S., Cohn, J. A., and Wilson, J. M. (1993) The common variant of cystic fibrosis transmembrane conductance regulator is recognized by hsp70 and degraded in a pre-Golgi nonlysosomal compartment, *Proc. Natl. Acad. Sci. U.S.A. 90*, 9480−9484.
21. Amara, J. F., Cheng, S. H., and Smith, A. E. (1992) Intracellular protein trafficking defects in human disease, *Trends Cell Biol. 2*, 145−149.
22. Lomas, D. A., Evans, D. L., Finch, J. T., and Carrell, R. W. (1992) The mechanism of Z alpha 1-antitrypsin accumulation in the liver, *Nature 357*, 605−607.
23. Sifers, R. N. (1992) Protein transport. Z and the insoluble answer, *Nature 357*, 541−542.
24. Rajaraman, K., Raman, B., and Rao, C. M. (1996) Molten-globule state of carbonic anhydrase binds to the chaperone-like alpha-crystallin, *J. Biol. Chem. 271*, 27595−27600.
25. Rawat, U., and Rao, M. (1998) Interactions of chaperone alpha-crystallin with the molten globule state of xylose reductase. Implications for reconstitution of the active enzyme, *J. Biol. Chem. 273*, 9415−9423.
26. Martin, J., Langer, T., Boteva, R., Schramel, A., Horwich, A. L., and Hartl, F. U. (1991) Chaperonin-mediated protein folding at the surface of groEL through a 'molten globule'-like intermediate, *Nature 352*, 36−42.
27. Robinson, C. V., Gross, M., Eyles, S. J., Ewbank, J. J., Mayhew, M., Hartl, F. U., Dobson, C. M., and Radford, S. E. (1994) Conformation of GroEL-bound alpha-lactalbumin probed by mass spectrometry, *Nature 372*, 646−651.
28. Song, M., Shao, H., Mujeeb, A., James, T. L., and Miller, W. L. (2001) Molten-globule structure and membrane binding of the N-terminal protease-resistant domain (63-193) of the steroidogenic acute regulatory protein (StAR), *Biochem. J. 356*, 151−158.
29. Ren, J., Kachel, K., Kim, H., Malenbaum, S. E., Collier, R. J., and London, E. (1999) Interaction of diphtheria toxin T domain with molten globule-like proteins and its implications for translocation, *Science 284*, 955−957.
30. van der Goot, F. G., Gonzalez-Manas, J. M., Lakey, J. H., and Pattus, F. (1991) A 'molten-globule' membrane-insertion intermediate of the pore-forming domain of colicin A, *Nature 354*, 408−410.
31. Bychkova, V. E., Pain, R. H., and Ptitsyn, O. B. (1988) The 'molten globule' state is involved in the translocation of proteins across membranes? *FEBS Lett. 238*, 231−234.
32. Jennings, P. A., and Wright, P. E. (1993) Formation of a molten globule intermediate early in the kinetic folding pathway of apomyoglobin, *Science 262*, 892−896.
33. Hughson, F. M., Wright, P. E., and Baldwin, R. L. (1990) Structural characterization of a partly folded apomyoglobin intermediate, *Science 249*, 1544−1548.
34. Jeng, M. F., Englander, S. W., Elove, G. A., Wand, A. J., and Roder, H. (1990) Structural description of acid-denatured cytochrome c by hydrogen exchange and 2D NMR, *Biochemistry 29*, 10433−10437.
35. Mizuguchi, M., Masaki, K., Demura, M., and Nitta, K. (2000) Local and long-range interactions in the molten globule state: A study of chimeric proteins of bovine and human alpha-lactalbumin, *J. Mol. Biol. 298*, 985−995.
36. Ogasahara, K., Matsushita, E., and Yutani, K. (1993) Further examination of the intermediate state in the denaturation of the tryptophan synthase alpha subunit. Evidence that the equilibrium denaturation intermediate is a molten globule, *J. Mol. Biol. 234*, 1197−1206.
37. Pfeil, W. (1998) Is the molten globule a third thermodynamic state of protein? The example of alpha-lactalbumin, *Proteins 30*, 43−48.
38. Pfeil, W., Bychkova, V. E., and Ptitsyn, O. B. (1986) Physical nature of the phase transition in globular proteins. Calorimetric study of human alpha-lactalbumin, *FEBS Lett. 198*, 287−291.
39. Yutani, K., Ogasahara, K., and Kuwajima, K. (1992) Absence of the thermal transition in apo-alpha-lactalbumin in the molten

globule state. A study by differential scanning microcalorimetry, *J. Mol. Biol. 228*, 347−350.
40. Marmorino, J. L., Lehti, M., and Pielak, G. J. (1998) Native tertiary structure in an A-state, *J. Mol. Biol. 275*, 379−388.
41. Sheshadri, S., Lingaraju, G. M., and Varadarajan, R. (1999) Denaturant mediated unfolding of both native and molten globule states of maltose binding protein are accompanied by large deltaCp's, *Protein Sci. 8*, 1689−1695.
42. Prajapati, R. S., Das, M., Sreeramulu, S., Sirajuddin, M., Srinivasan, S., Krishnamurthy, V., Ranjani, R., Ramakrishnan, C., and Varadarajan, R. (2006) Thermodynamic effects of proline introduction on protein stability, *Proteins 66*, 480−491.
43. Magnusson, U., Salopek-Sondi, B., Luck, L. A., and Mowbray, S. L. (2004) X-ray structures of the leucine-binding protein illustrate conformational changes and the basis of ligand specificity, *J. Biol. Chem. 279*, 8747−8752.
44. Prajapati, R. S., Sirajuddin, M., Durani, V., Sreeramulu, S., and Varadarajan, R. (2006) Contribution of cation-pi interactions to protein stability, *Biochemistry 45*, 15000−15010.
45. Ganesh, C., Shah, A. N., Swaminathan, C. P., Surolia, A., and Varadarajan, R. (1997) Thermodynamic characterization of the reversible, two-state unfolding of maltose binding protein, a large two-domain protein, *Biochemistry 36*, 5020−5028.
46. Pace, C. N., Vajdos, F., Fee, L., Grimsley, G., and Gray, T. (1995) How to measure and predict the molar absorption coefficient of a protein, *Protein Sci. 4*, 2411−2423.
47. Milev, S., Bjelic, S., Georgiev, O., and Jelesarov, I. (2007) Energetics of peptide recognition by the second PDZ domain of human protein tyrosine phosphatase 1E, *Biochemistry 46*, 1064−1078.
48. Connelly, P. R., Varadarajan, R., Sturtevant, J. M., and Richards, F. M. (1990) Thermodynamics of protein-peptide interactions in the ribonuclease S system studied by titration calorimetry, *Biochemistry 29*, 6108−6114.
49. Quiocho, F. A., Spurlino, J. C., and Rodseth, L. E. (1997) Extensive features of tight oligosaccharide binding revealed in high-resolution structures of the maltodextrin transport/chemosensory receptor, *Structure 5*, 997−1015.
50. Sharff, A. J., Rodseth, L. E., Spurlino, J. C., and Quiocho, F. A. (1992) Crystallographic evidence of a large ligand-induced hinge-twist motion between the two domains of the maltodextrin binding protein involved in active transport and chemotaxis, *Biochemistry 31*, 10657−10663.
51. Trakhanov, S., Vyas, N. K., Luecke, H., Kristensen, D. M., Ma, J., and Quiocho, F. A. (2005) Ligand-free and -bound structures of the binding protein (LivJ) of the *Escherichia coli* ABC leucine/isoleucine/valine transport system: trajectory and dynamics of the interdomain rotation and ligand specificity, *Biochemistry 44*, 6597−6608.
52. Myers, J. K., Pace, C. N., and Scholtz, J. M. (1995) Denaturant m values and heat capacity changes: relation to changes in accessible surface areas of protein unfolding, *Protein Sci. 4*, 2138−2148.
53. Hubbard, S. J., and Thronton, J. M. (1993) *NACCESS*, Computer Program, Department of Biochemistry and Molecular Biology, University College, London, England.
54. Fukada, H., Sturtevant, J. M., and Quiocho, F. A. (1983) Thermodynamics of the binding of L-arabinose and of D-galactose to the L-arabinose-binding protein of *Escherichia coli*, *J. Biol. Chem. 258*, 13193−13198.
55. Bajaj, K., Chakshusmathi, G., Bachhawat-Sikder, K., Surolia, A., and Varadarajan, R. (2004) Thermodynamic characterization of monomeric and dimeric forms of CcdB (controller of cell division or death B protein), *Biochem. J. 380*, 409−417.
56. Chimienti, M., Moizi, M., Salerno, J. A., Klersy, C., Guasti, L., Previtali, M., Marangoni, E., Montemartini, C., and Bobba, P. (1987) Electrophysiologic and clinical effects of intravenous and oral encainide in patients with Wolff-Parkinson-White syndrome and paroxysmal atrial fibrillation, *Eur. Heart J. 8*, 282−290.
57. Dolgikh, D. A., Abaturov, L. V., Bolotina, I. A., Brazhnikov, E. V., Bychkova, V. E., Gilmanshin, R. I., Lebedev, Yu, O., Semisotnov, G. V., Tiktopulo, E. I., Ptitsyn, O. B., et al. (1985) Compact state of a protein molecule with pronounced small-scale mobility: bovine alpha-lactalbumin, *Eur. Biophys. J. 13*, 109−121.
58. Kuwajima, K. (1977) A folding model of alpha-lactalbumin deduced from the three-state denaturation mechanism, *J. Mol. Biol. 114*, 241−258.
59. Ptitsyn, O. B. (1995) Molten globule and protein folding, *Adv. Protein Chem. 47*, 83−229.
60. Semisotnov, G. V., Rodionova, N. A., Razgulyaev, O. I., Uversky, V. N., Gripas, A. F., and Gilmanshin, R. I. (1991) Study of the "molten globule" intermediate state in protein folding by a hydrophobic fluorescent probe, *Biopolymers 31*, 119−128.
61. Griko, Y. V. (2000) Energetic basis of structural stability in the molten globule state: alpha-lactalbumin, *J. Mol. Biol. 297*, 1259−1268.
62. Xie, D., Bhakuni, V., and Freire, E. (1991) Calorimetric determination of the energetics of the molten globule intermediate in protein folding: apo-alpha-lactalbumin, *Biochemistry 30*, 10673−10678.
63. Koshiba, T., Hayashi, T., Miwako, I., Kumagai, I., Ikura, T., Kawano, K., Nitta, K., and Kuwajima, K. (1999) Expression of a synthetic gene encoding canine milk lysozyme in *Escherichia coli* and characterization of the expressed protein, *Protein Eng. 12*, 429−435.
64. Griko, Y. V., Freire, E., Privalov, G., van Dael, H., and Privalov, P. L. (1995) The unfolding thermodynamics of c-type lysozymes: a calorimetric study of the heat denaturation of equine lysozyme, *J. Mol. Biol. 252*, 447−459.
65. Carra, J. H., Anderson, E. A., and Privalov, P. L. (1994) Thermodynamics of staphylococcal nuclease denaturation. II. The A-state, *Protein Sci. 3*, 952−959.
66. Qureshi, S. H., Moza, B., Yadav, S., and Ahmad, F. (2003) Conformational and thermodynamic characterization of the molten globule state occurring during unfolding of cytochromes-c by weak salt denaturants, *Biochemistry 42*, 1684−1695.
67. Hagihara, Y., Tan, Y., and Goto, Y. (1994) Comparison of the conformational stability of the molten globule and native states of horse cytochrome c. Effects of acetylation, heat, urea and guanidine-hydrochloride, *J. Mol. Biol. 237*, 336−348.
68. Privalov, P. L., and Gill, S. J. (1988) Stability of protein structure and hydrophobic interaction, *Adv. Protein Chem. 39*, 191−234.
69. Murphy, K. P., and Gill, S. J. (1991) Solid model compounds and the thermodynamics of protein unfolding, *J. Mol. Biol. 222*, 699−709.
70. Privalov, P. L., and Makhatadze, G. I. (1990) Heat capacity of proteins. II. Partial molar heat capacity of the unfolded polypeptide chain of proteins: protein unfolding effects, *J. Mol. Biol. 213*, 385−391.
71. Hamada, D., Kidokoro, S., Fukada, H., Takahashi, K., and Goto, Y. (1994) Salt-induced formation of the molten globule state of cytochrome c studied by isothermal titration calorimetry, *Proc. Natl. Acad. Sci. U.S.A. 91*, 10325−10329.
72. Nakamura, S., and Kidokoro, S. (2005) Direct observation of the enthalpy change accompanying the native to molten-globule transition of cytochrome c by using isothermal acid-titration calorimetry, *Biophys. Chem. 113*, 161−168.
73. Griko, Y. V., and Privalov, P. L. (1994) Thermodynamic puzzle of apomyoglobin unfolding, *J. Mol. Biol. 235*, 1318−1325.
74. Wu, L. C., and Kim, P. S. (1998) A specific hydrophobic core in the alpha-lactalbumin molten globule, *J. Mol. Biol. 280*, 175−182.
75. Peng, Z. Y., Wu, L. C., Schulman, B. A., and Kim, P. S. (1995) Does the molten globule have a native-like tertiary fold? *Philos. Trans. R. Soc. London, Ser. B 348*, 43−47.
76. Gebhard, L. G., Risso, V. A., Santos, J., Ferreyra, R. G., Noguera, M. E., and Ermacora, M. R. (2006) Mapping the distribution of conformational information throughout a protein sequence, *J. Mol. Biol. 358*, 280−288.
77. Spurlino, J. C., Lu, G. Y., and Quiocho, F. A. (1991) The 2.3-A resolution structure of the maltose- or maltodextrin-binding protein, a primary receptor of bacterial active transport and chemotaxis, *J. Biol. Chem. 266*, 5202−5219.
78. Andreeva, A., Howorth, D., Brenner, S. E., Hubbard, T. J., Chothia, C., and Murzin, A. G. (2004) SCOP database in 2004: refinements integrate structure and sequence family data, *Nucleic Acids Res. 32*, D226−D229.
79. Murzin, A. G., Brenner, S. E., Hubbard, T., and Chothia, C. (1995) SCOP: a structural classification of proteins database for the investigation of sequences and structures, *J. Mol. Biol. 247*, 536−540.
80. Beena, K., Udgaonkar, J. B., and Varadarajan, R. (2004) Effect of signal peptide on the stability and folding kinetics of maltose binding protein, *Biochemistry 43*, 3608−3619.

BI700577M